Available online at www.sciencedirect.com
SCIENCE DIRECT®
Scripta Materialia 53 (2005) 207–212
Scripta MATERIALIA
www.actamat-journals.com

EBSD study of grain subdivision of a Goss grain in coarse-grained cold-rolled niobium

H.R.Z. Sandim [a,*], D. Raabe [b]

[a] Department of Materials Engineering, FAENQUIL, P.O. Box 116, 12600-970 Lorena, Brazil
[b] Max-Planck-Institut für Eisenforschung, Max-Planck Strasse 1, D-40237 Düsseldorf, Germany

Received 9 February 2005; received in revised form 14 March 2005; accepted 23 March 2005
Available online 25 April 2005

Abstract

Deformation-driven grain subdivision of three neighboring grains is investigated in 80% cold-rolled coarse-grained niobium using high-resolution electron backscatter diffraction. Particular focus is placed on the study of the deformation-induced grain fragmentation of a Goss-oriented crystal.

Keywords: Orientation gradient; Niobium; Grain subdivision; EBSD; Inhomogeneous deformation

1. Introduction

The microstructure of as-cast high-purity niobium ingots processed by electron beam melting mostly consists of a few large columnar grains of cm-size. The ensuing plastic deformation of such coarse-grained materials usually leads to a very inhomogeneous deformation microstructure [1,2]. Both the gradual grain subdivision during deformation and corresponding nucleation effects observed during further heat treatment of such coarse-grained refractory metals like niobium, tantalum, and molybdenum [3–7] were reported earlier to depend strongly on the initial crystallographic orientation of such large grains. Similar observations that document the orientation dependence of deformation induced grain subdivision (and, in part, of the subsequent recrystallization) were also reported for iron [8–13]. In many cases, the substructure was observed to vary from one grain to another, particular with respect to the overall orientation gradient building up gradually during straining within the original grain borders. It is obvious that a good understanding of the relationship between grain orientation and grain fragmentation behavior is a prerequisite to understanding deformation heterogeneity in coarse-grained metals [8,14,15].

High-resolution electron backscatter diffraction (EBSD) in conjunction with a field emission gun scanning electron microscope (FEG-SEM) is a useful analytical tool in that context in that it allows one to study in-grain orientation gradient effects at the mesoscopic scale down to a lateral resolution of about 20 nm at an improved angular resolution [16,17]. Furthermore, the FEG-SEM/EBSD method allows one to study orientation gradients over large areas more easily than in the transmission electron microscope. This latter aspect is of particular relevance when it comes to the investigation of in-grain texture changes in large crystals. On the other hand, the FEG-SEM/EBSD method is not well suited to distinguish in high detail blurred orientation changes below 1–2° which extend over a smeared out subgrain wall.

* Corresponding author. Tel.: +55 12 3159 9916; fax: +55 12 3153 3006.
E-mail address: hsandim@demar.faenquil.br (H.R.Z. Sandim).

1359-6462/$ - see front matter
doi:10.1016/j.scriptamat.2005.03.045

The present paper presents experimental results on deformation-induced grain subdivision in three neighboring coarse grains in a 80% cold-rolled niobium specimen using the FEG-SEM/EBSD technique. The results reveal noticeable differences in terms of grain fragmentation and microstructural development. Of particular interest is the fragmentation of a large Goss-oriented grain, which can be described in terms of symmetric orientation changes about the transverse crystal direction.

2. Experimental

A high-purity coarse-grained niobium ingot was prepared by multiple electron beam melting (EBM). Interstitial (O < 50, N < 5, wt ppm) and metallic (W < 55, Fe < 45, Al < 30 and Si < 50 wt ppm) impurity contents are in agreement with ASTM-B-391-99 (reactor-grade purity). In the initial state the ingot consisted of columnar grains with grain boundaries lying nearly parallel to the rolling direction. These grains were 10–30 mm wide and 40–200 mm long. A thick slab (50 mm thickness × 140 mm width × 300 mm length) was cut from the center of the ingot. Subsequent cold rolling was conducted to a total engineering thickness reduction of 80% (corresponding to a true strain of $\varepsilon = 1.6$). Three adjacent grains were sampled in the longitudinal section of the rolled plate. Metallographic preparation of the sections was carried out using conventional techniques including repeated chemical polishing to remove surface deformation. Vickers microhardness tests were carried out using a load of 50 g. The results presented correspond to the mean value of 15 values taken on each specimen. The microstructures of the deformed and annealed specimens (900 °C, 1 h) were observed in detail in a JEOL JSM-6500F FEG-SEM operating at 15 kV [18]. The EBSD scans were carried out in areas of about $120 \times 50\ \mu m^2$ in the longitudinal plane (RD-ND plane) at the grain boundary region in the rolled specimens. In the following presentations RD refers to the rolling direction, TD to the transverse direction, and ND to the normal direction of the rolled sheet. EBSD sampling points were taken in 100 nm steps (corresponding to the texture map step size). Microtexture evaluation was conducted by means of automated acquisition and further indexing of Kikuchi patterns after suitable image processing in a TSL system interfaced to the FEG-SEM [12,18]. Owing to the high reduction and the large stored energy the mapping speed varied from 10 to 15 patterns per second. Pole figures and misorientation (ψ) distributions were determined for each mapped region. Adjacent areas of each grain in the vicinity of the prior grain boundary were scanned to allow us to compare the grains. In the following these two interfaces are referred to as A–B and B–C.

3. Results

The microstructure of 80% cold-rolled niobium displays elongated grains with grain boundaries aligned nearly parallel to the RD. Assuming an initial grain size in ND of about 10 mm prior to rolling, one expects that the original grains have thinned to about 2 mm thickness. It is important to mention in that context that the cross section of the 150-mm diameter EBM niobium ingots consists of only a few grains, usually 10–20 across the diameter. Therefore, it is pertinent to underline that the microstructure of individual grains plays an important role in the overall mechanical behavior of such samples. The hardness varied for grains A, B, and C after rolling. The results of the mean Vickers hardness found in these grains were 122, 130, and 136, respectively.

The substructure developed after cold rolling differs markedly between the different grains. Fig. 1 shows the three crystals as seen in the SEM. Although the channeling contrast cannot resolve all relevant details of the microstructure it allows one to study relative misorientations of about 1° at a lateral resolution of 1 μm. The Kikuchi patterns obtained during FEG-SEM/EBSD measurements were very sharp easing further computer-assisted orientation indexing. Large mappings of about $60 \times 50\ \mu m^2$ were performed in each grain. Taking into account the predicted grain size for this material after 80% cold rolling, the results shown in this paper represent the behavior of these grains at their respective grain boundary regions.

Grains A and C developed lamellar microstructures with bands nearly parallel to RD. Grain B, on the other hand, developed a coarser structure. Bands of localized shear making about 45° with respect to RD are present subdividing the microstructure of grain B. A fairly organized subgrain structure is found in grain B. These bands are very diffuse in the orientation image map and can only be distinguished by shading among different regions corresponding to low local lattice misorientations.

The differences in terms of grain subdivision and developed misorientations were quantified on the basis of the FEG-SEM/EBSD measurements. Orientation maps from EBSD data are shown in Fig. 2. They reveal differences concerning grain subdivision of the three grains. The transition from one grain to another can be easily distinguished in grain boundary A–B. In a contrasting manner, boundary B–C displays a narrow transition zone of about 20 μm where the original grain boundary cannot be easily recognized, at least at first sight. Grain A, on the other hand, shows narrow bands, 1–2 μm spaced, and lying parallel to RD. The misorientation across these bands is typically above 40° as found also for grain C.

Fig. 3 displays the boundary misorientation distributions determined in grains A, B, and C. Only boundaries

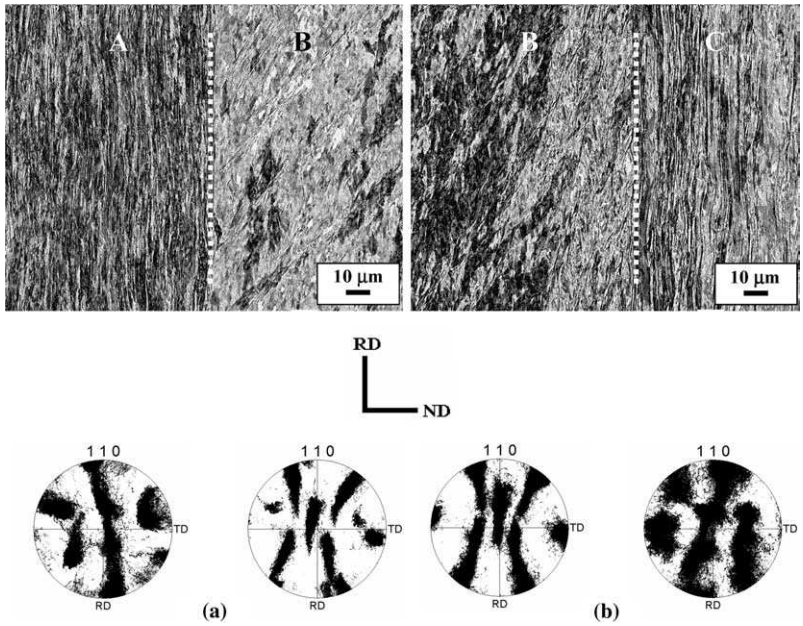

Fig. 1. Longitudinal sections of grains A, B, and C showing the microstructures and corresponding pole figures in 80% cold-rolled niobium (FEG-SEM, backscattered electrons): (a) boundary A–B; (b) boundary B–C. Grain boundary (dashed line) lies nearly in the center of each micrograph.

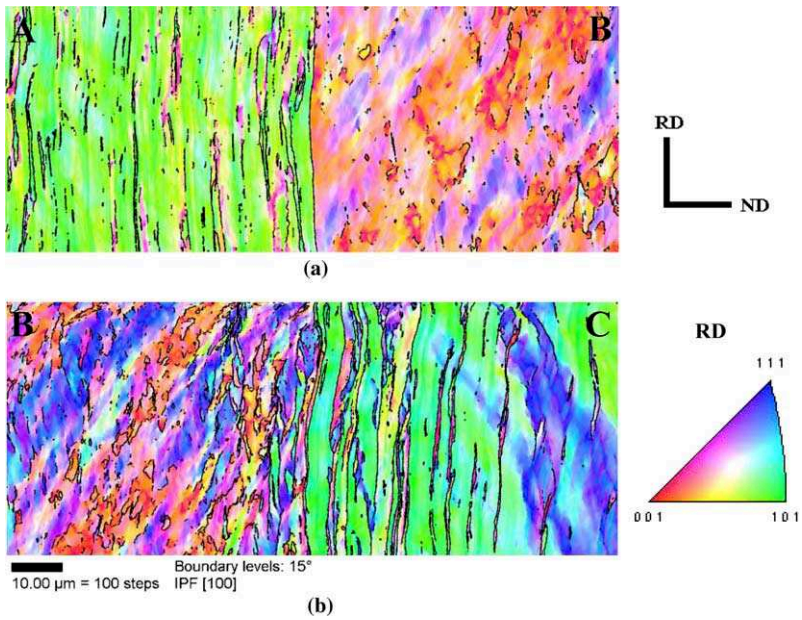

Fig. 2. Orientation maps showing details of the grain boundary region of: (a) grains A and B; (b) grains B and C. Color coded map referred to RD is shown at right side. Fine black lines mark high-angle boundaries.

with $\psi > 2°$ are shown in the histograms. Misorientations below 5° are marked as black bins. The distributions are based on data taken from equal-sized areas in each of the grains investigated. The results from boundary A to B indicate that grain A has subdivided into a wide range of misorientations with many boundaries having high angle character ($\psi > 15°$). The spacing among high angle boundaries in grain A was found to be about 2.1 μm using the linear intercept method. Grain B did not develop a fully lamellar structure. Low angle grain boundaries are most predominant in grain B ($2° < \psi < 10°$). No secondary high angle peak was observed for grain B. Grain C contains a larger fraction of high angle boundaries compared to grains A and B, especially those above 50°. The spacing between high angle boundaries, in this case, was slightly smaller, close to 1.6 μm. However, it should be noted that the first two bins corresponding to misorientations below 5°

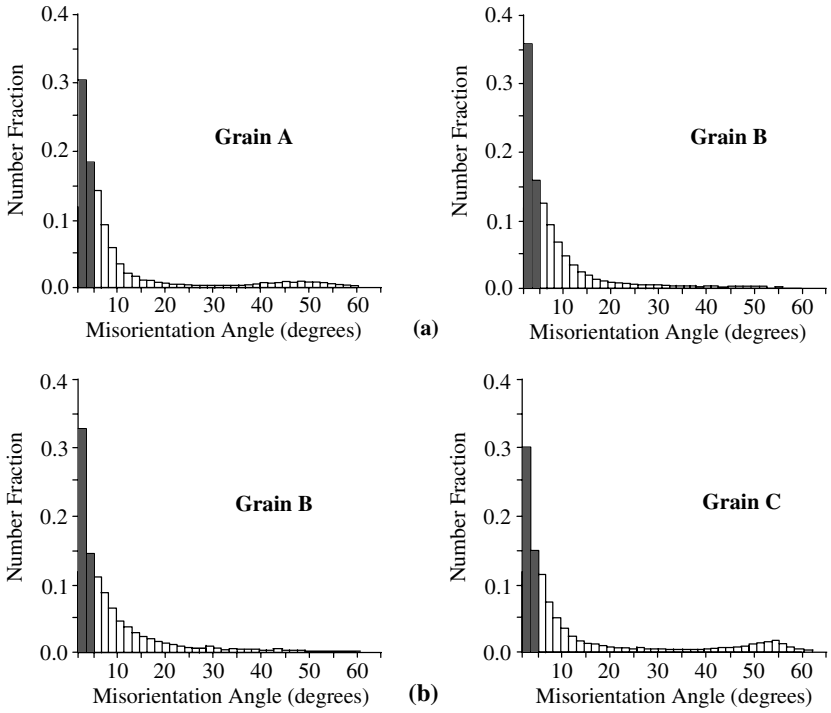

Fig. 3. Boundary misorientation distribution determined in transverse section of grains A, B, and C from FEG-SEM/EBSD measurements in boundaries: (a) A–B; (b) B–C.

for grains A, B, and C add up to values whose differences are not particularly large.

In agreement with the differences found in the deformed state, strong local differences in the rate of static recrystallization were observed. Fig. 4 shows the microstructure of a region comprising grains A, B, and C after annealing at 900 °C for 1 h. Recrystallization was incomplete in grain A. The new grains display an elongated morphology and were nucleated preferentially at the highly misoriented bands shown in Fig. 2a. Grain B, on the other hand, displayed a higher recrystallized volume fraction ($X_{RX} > 90\%$). The recrystallized grain size in this case was about 90 μm. Completed recrystallization was observed in the former grain C. Fig. 4 shows a fine equiaxed structure with a grain size close to 30 μm on the right side.

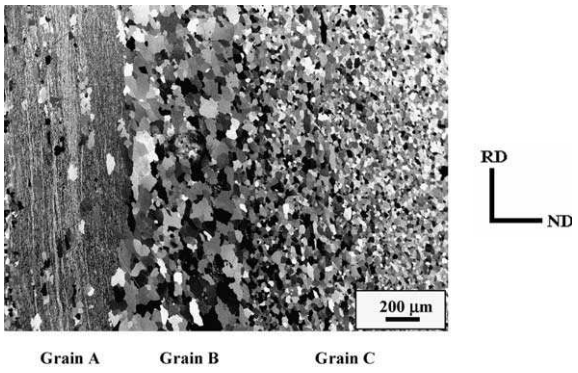

Fig. 4. Longitudinal sections of former grains A, B, and C showing their respective microstructures after annealing at 900 °C for 1 h (FEG-SEM, backscattered electrons). Position of former grains A, B, and C is indicated.

4. Discussion

The grain-to-grain heterogeneity in terms of the deformation structure in these coarse grains is evident. The microstructural evolution of niobium during cold rolling can be described in terms of grain subdivision by generation of geometrically necessary boundaries to accommodate the increasing local lattice misorientations [2,19]. In a previous paper, the heterogeneity of the deformation microstructure in coarse-grained tantalum deformed by cold swaging was reported [4]. In that study, distinct substructures (lamellar and non-lamellar ones) were found to vary from one grain to another indicating a significant influence of the initial grain orientation. This heterogeneity is also present in cold-rolled niobium with an initial coarse-grained structure. Prior SEM (electron channeling contrast) and conventional EBSD measurements (W-filament) reported the dependence of the nature of the cold-worked structure with initial grain orientation in niobium bicrystals [3] and also oligocrystals [20]. The presence of fully lamellar microstructures developed in grains A and C at large strains are in agreement with those described by the grain subdivision model developed for medium-to-high stacking fault energy metals [19,21]. At large strains

($\varepsilon \approx 1.5$–2), most of these dislocation boundaries tend to reorient into a lamellar structure having a wide range of misorientations, many of them with high angle character [21,22]. This model is based on extensive TEM studies conducted on thin foils of deformed metals including single and polycrystalline specimens. The tendency of grain subdivision into lamellae of strongly different orientations is also distinctly orientation-dependent [23]. Lamellar structures are observed in grains A and C but not in grain B (see Figs. 1 and 2) supporting this dependence on the initial orientation of each grain (unknown in the present case). Nevertheless, it is worthwhile mentioning that there is much less data in the literature concerning the development of lamellar structures in coarse-grained materials than in fine-grained ones.

The initial orientation of grain B was most likely Goss ($\{0\,1\,1\}\ \langle 0\,0\,1\rangle$). Orientations close to the Goss-component in body-centered cubic materials are indeed known to be very unstable under plane strain loading [23]. Grain B rotates slightly about TD from one boundary to another. One important result, which has not been observed before in experiments in this context, is the orientation spread occurring in grain B (see the two pole figures shown in Figs. 1a and b). The data in the $\{1\,1\,0\}$-pole figure reveal a strong orientation spread about the Goss, which is characterized by two symmetric orientation branches, which are related to each other by a rotation about the transverse direction. In a recent theoretical treatment [23] orientations close to the Goss were indeed predicted to undergo such an orientation split under plane strain loading. The predictions were made using both homogenization theory and a crystal plasticity finite element approach. The theoretical treatment for the prediction of in-grain orientation gradients was essentially built on the divergence of the re-orientation fields of the respective texture component.

Fig. 5a shows the in-grain texture in a deformed Goss crystal of a body centered cubic material under plane strain loading in the form of a $\{1\,1\,1\}$-pole figure. The open squares show the initial orientation (which is the same at all integration points) and the black dots show the orientations after deformation. The deformed grain is characterized using the accumulated misorientations in a gray scale coding (light values indicate large misorientations). These data are compared with crystal plasticity finite element simulations conducted using 48 slip systems to a thickness reduction of 50% (Fig. 5b). Although there is no direct experimental evidence that grain B was initially Goss-oriented, the $\{1\,1\,1\}$-pole figure corresponding to this grain in the deformed state (Fig. 5c) look very similar to those obtained from the finite element plasticity model. Thus, experimental results combined to those obtained from finite element modeling confirm this behavior is typical of Goss-oriented grains.

Annealing at low homologous temperatures is a useful method to investigate possible orientation effects on recovery and recrystallization in coarse-grained materials. Important aspects like recrystallized grain size, recrystallized volume fraction, and preferential nucleation sites (grain boundaries and/or deformation heterogeneities) can be investigated in detail by means of such a procedure. The results shown in this paper confirm the inhomogeneity of the annealed state in oligocrystalline niobium. The microstructure presented in Fig. 4 consists of regions whose widths mark the presence of individual grains. These distinct regions display partial or full recrystallization with large local variations in grain size. Recrystallization in former grain A was partial. The nucleation of the new grains is chiefly associated to the 40°-misoriented bands lying parallel to the RD. The typical misorientations found in regions far from these bands were about 10° or even smaller. Contrarily, the finer grain size found in former grain C has probably to do with the slightly higher fraction of high-angle boundaries in the deformed state, especially those above 45°. Grain B displayed an intermediary behavior compared to grains A and C. Recrystallization was also partial and a few recovered areas are still visible within grain B. Its coarser grain structure in the annealed state can be explained by the presence of a lesser number of potential nucleation sizes but, contrasting with grain A, an advantage in terms of growth is evident. It can

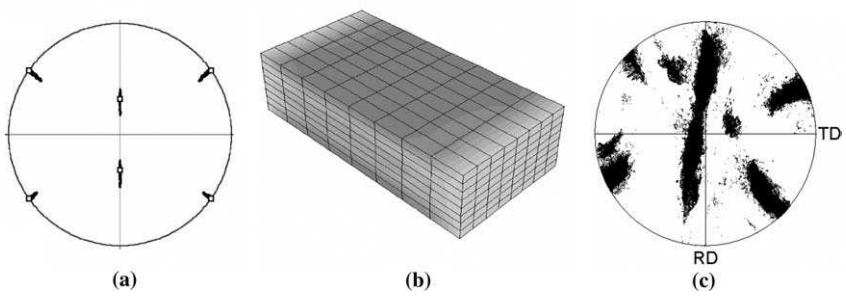

Fig. 5. In-grain texture in a deformed Goss crystal of a body centered cubic material under plane strain loading: (a) $\{1\,1\,1\}$-pole figure, 48 slip systems, and thickness reduction of 50%; (b) gray scale coding indicates accumulated misorientations; (c) $\{1\,1\,1\}$-pole figure corresponding to grain B after thickness reduction of 80%.

be noticed in Fig. 3 that the amount of boundaries with low angle character in grain B, especially those below 5°, is only slightly larger compared to the distributions for grains A and C. A measure of the stored energy in the deformed state could be estimated by use of the average values of the boundary spacing and misorientation angles. However, misorientation distributions alone cannot completely explain the recrystallization behavior found in these grains. The spatial arrangement of these misorientations in the deformed microstructure must be also taken into account and further experimental work is needed to clarify this important point.

5. Conclusions

The results shown in the present work confirm the strong mesoscale heterogeneity of the deformation structure in coarse-grained niobium. The microstructure of 80% cold-rolled niobium reveals noticeable differences in terms of grain subdivision from one grain to another. Channeling contrast for FEG-SEM combined with orientation mappings provided by high-resolution field emission EBSD measurements were used to characterize the microstructure. Boundary misorientation distributions were determined for three distinct grains at their respective grain boundary regions. Results show noticeable differences in terms of fragmentation and misorientations developed in grains A and C (full lamellar structures) compared to grain B (non-lamellar structure).

Acknowledgments

The authors acknowledge CAPES-DAAD for providing support for this work. The kind assistance of Mrs. Katja Angenendt (MPI-E, Düsseldorf) in FEG-SEM-EBSD is also acknowledged. H.R.Z. Sandim is supported by CNPq (Brazil).

References

[1] Hansen N. Metall Trans 1985;16A:2167.
[2] Hansen N. Mater Sci Technol 1990;6:1039.
[3] Sandim HRZ, Lins JFC, Pinto AL, Padilha AF. Mater Sci Eng 2003;354A:217.
[4] Sandim HRZ, McQueen HJ, Blum W. Scripta Mater 1999;42:151.
[5] Raabe D, Lücke K, Gottstein G. J Phys IV, colloque C7, supplément au J Phys III 1993;3:523.
[6] Raabe D, Schlenkert G, Weisshaupt H, Lücke K. Mater Sci Technol 1994;10:229.
[7] Raabe D, Lücke KZ. Metallkde 1994;85:302.
[8] Hölscher M, Raabe D, Lücke K. Steel Res 1991;62:567.
[9] Raabe D. Phys Status Solidi (b) 1994;181:291.
[10] Raabe D. Steel Res 1995;66:222.
[11] Raabe D. Scripta Metall 1995;33:735.
[12] Thomas I, Zaefferer S, Friedel F, Raabe D. Adv Eng Mater 2003;5:566.
[13] Li BL, Godfrey A, Liu Q. Scripta Mater 2004;50:879.
[14] Poulsen HF, Margulies L, Schmidt S, Winther G. Acta Mater 2003;51:3821.
[15] Winther G, Margulies L, Schmidt S, Poulsen HF. Acta Mater 2004;52:2863.
[16] Mishin OV, Huang X, Bowen JR, Juul Jensen D. In: Dinesen AR, Eldrup M, Juul Jensen D, Linderoth S, Pedersen TB, Pryds NH, et al., editors. Proceedings of the 22nd Risø International Symposium on Materials Science, Risø National Laboratory, Roskilde, Denmark, 2001. p. 335.
[17] Isabell TC, Dravid VP. Ultramicroscopy 1997;67:59.
[18] Zaefferer S, Kuo J-C, Zhao Z, Winning M, Raabe D. Acta Mater 2003;51:4719–35.
[19] Bay B, Hansen N, Kuhlmann-Wilsdorf D. Mater Sci Eng 1992;158A:139.
[20] Lins JFC. Dissertation, FAENQUIL, Lorena, 2002.
[21] Hughes DA, Hansen N. Metall Trans 1993;24A:2021.
[22] Hughes DA, Hansen N. Acta Mater 1997;45:3871.
[23] Raabe D, Zhao Z, Park S-J, Roters F. Acta Mater 2002;50:421.